Experimental Verification of a One-turn Transformer Power Supply Circuit for Gate Drive Unit

Jun-ichi Itoh, Takeshi Kinomae

*Nagaoka University of Technology/Department of Electrical, Electronics and Information Engineering,
Nagaoka, Japan, e-mail: itoh@vos.nagaokaut.ac.jp, kinome@stn.nagaokaut.ac.jp

Abstract — **This paper proposes a power supply circuit for gate drive units (GDU) that uses a one-turn transformer which is given advantages in term of cost and loss. The structure of this one–turn transformer consists of one turn in the primary winding and multiple turns in the secondary winding. Then the circuit is connected in series to a main switching device to obtain a power for the GDUs. The proposed circuit can be applied to all kinds of main circuit topologies such as a multi-level converter topology or a matrix converter in addition to a conventional 6-arm inverter. In this paper, the design method of the one-turn transformer and the characteristics are described accordingly based on the fundamental experimental results. Besides, the proposed circuit with GDUs is tested in a three-phase inverter for verification purpose. The results confirmed that the proposed gate drive circuit is working without an external power source circuit when the output current is 1/10 times over the rated current of the switching device.**

Keywords —**Power supplies, Power transformer Gate Drive Unit,**

I. INTRODUCTION

A gate drive unit (GDU) is generally used for power converters to operate the switching devices such as IGBT, MOS-FET and others [1-4]. The GDUs required additional power supply units because the electric potential of emitter of the switching device is difference depending on the switching device in the main circuit.

Generally, an isolated DC-DC converter is used for a gate power supply; however extra cost is implemented. There are some design approaches for cost reduction, such as a charge pump circuit, a bootstrap circuit, and a self-supplying power circuit using a series regulator [5-8]. The bootstrap circuit has a simple configuration, and the charge pump circuit can reduce the volume of the capacitor, furthermore these two circuits can be applied easily to a conventional inverter topology.

However, when these two circuits apply to other main circuit topologies such as matrix converters or multi-level converters, several problems are encountered. The number of parts in the gate power supply will increase [8], furthermore the voltage rating of the components in the gate power supply are depended on that of the main circuits.

On the other hand, the self-supplying power circuit using a series regulator provides some advantages in comparison to other two circuits. This gate power supply does not require high voltage rating parts as the other two circuits. In addition, the configuration of the gate power supply is not influenced by the main circuit, so this circuit can be accepted in all kinds of main circuit topologies. However, a large loss occurs at the series regulator in the self-supplying power circuit.

This paper proposes a self-supplying type of gate power circuit by using a transformer, which has a one-turn coil in the primary side. The purpose of the proposed circuit is achieving the cost reduction and low power loss in the gate power circuit.

The proposed gate power supply delivers the following features;

- The proposed circuit is isolated from the main circuit;
- The voltage rating of the components does not depend on the main circuit;
- An easy configuration that is composed of a transformer and a rectifier.
- A complicated control is unnecessary.

However, the output power of the transformer depends on the primary current and the switching frequency of the main circuit. In addition, these characteristics of the proposed circuits are analyzed and confirmed with a steady operation.

At first, this paper describes the characteristics of the one-turn coil transformer with an equivalent circuit. Then, the design method of a transformer is established. Secondly, the power supply characteristic for the GDU is investigated by experimented with a step-down chopper. Thirdly, the optimization of the connection point of the proposed transformer in a three-phase inverter is discussed. Finally, the experimental results from an inverter with the proposed self-supplying gate power circuit will be demonstrated.

II. INVESTIGATION OF ONE-TURN TRANSFORMER

This chapter shows an equivalent circuit of the one-turn coil transformer, then the adequacy of the equivalent circuit is verified by simulation results and experimental results.

A. Identification of equivalent circuit parameters

Fig. 1 shows the basic configuration of the proposed self-supplying power circuit is connecting to a step-down chopper. The proposed circuit consists of a diode rectifier and a transformer using one-turn coil in the primary side. The output power P_2 is supplied to the GDU. Note that a resistor is connected instead of a GDU in order to investigate the characteristics of the proposed circuit. The power consumption of the proposed power circuit is lower than the conventional series regulated self-supplying power

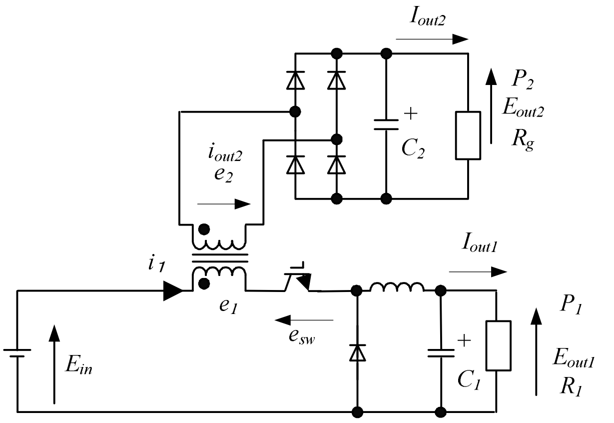

Fig.1. Experimental circuit for the proposed self supplying using one-turn transformer.

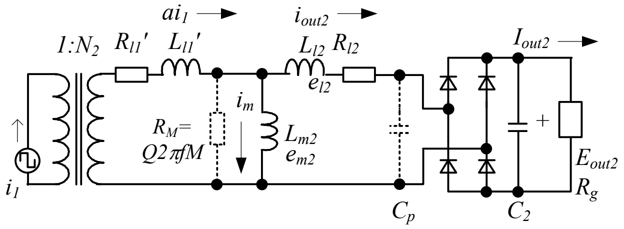

Fig. 2. Equivalent circuit with the secondary side mode of the transformer.

circuit because the step-down function of the voltage in the proposed circuit is implemented by a transformer instead of a series regulator.

Fig. 2 shows an equivalent circuit with the secondary side model of the transformer. The equivalent circuit is composed by an ideal transformer and T type circuit, which is expressed by a mutual inductance, leakage inductance and winding resistances. The primary side of the transformer is connected with a current source as the primary current.

The identification of the circuit parameter is obtained as following. At first, the compositional leakage inductance L_{sc2} on the secondary side is measured by a LCR meter when the primary side terminal is shorted. In addition, the secondary side self inductance L_2 is obtained by a LCR meter when the primary side terminal is opened. Then, the coupling factor k of the transformers is defined by

$$k = \sqrt{1 - L_{SC2}/L_2} \quad (1).$$

The mutual inductance L_{m2} in the equivalent circuit is obtained by

$$L_{m2} = kL_2 = \sqrt{k^2 \left(\frac{N_2}{N_1}\right)^2 L_1 L_2} \quad (2),$$

where N_1 is the number of primary winding turns, N_2 is the number of secondary winding turns.

On the other hand, the primary leakage inductance L_{l1}', which is transformed to the secondary side from the primary side, and the secondary leakage inductance L_{l2} are expressed by

$$L_{l2} = L_{l1}' = \left(\frac{N_2}{N_1}\right)^2 L_1(1-k) = L_2(1-k) \quad (3).$$

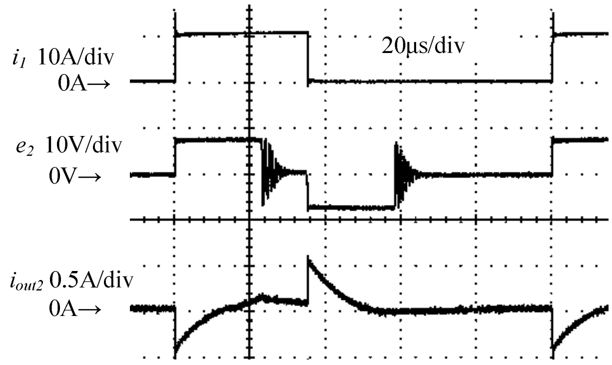

Fig. 3. Operation waveforms of proposed circuit. (f_{sw}=10 kHz, N_2=20 turn, *Duty*=35 %, I_{out1}=10 A).

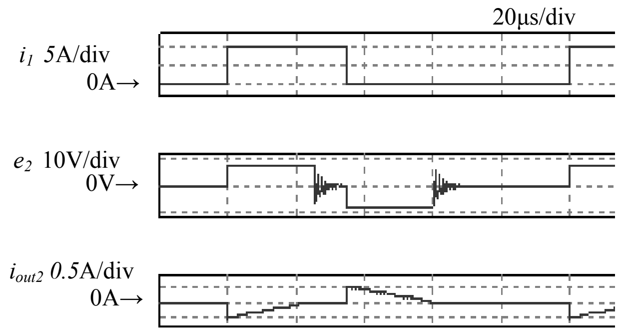

Fig. 4. Operation waveforms of equivalent circuit (f_{sw}=10 kHz, N_2=20 turn, *Duty*=35 %, I_{out1}=10 A).

B. Comparison of experimental waveforms with a simulation waveforms

Fig. 3 shows the waveforms of the secondary side output voltage e_2 and the secondary side current i_{out2} with the primary current i_1. The experimental conditions are; the step down chopper switching frequency f_{sw}=10 kHz, *Duty*=35%, output current I_{out1}=10 A, the coupling factor k=0.92, the number of secondary winding turn N_2=20 turn, mutual inductance L_{m2}=440 μH.

Fig. 4 shows the simulation waveforms by using the equivalent circuit as shown in Fig. 2. The simulation conditions are the same as the experimental conditions. From Fig.4, the simulation waveforms are similar to the experimental waveforms. The secondary voltage waveform e_2 is oscillating rapidly at two points; when the positive voltage is reducing to zero and when the negative voltage is returning to zero.

The oscillation frequency in e_2 at the first point (positive voltage) is different to that of e_2 at the second point (negative voltage). At the first point, the leakage inductance L_{sc2} appears in the secondary side because the induced electromotive force becomes zero since the primary current is constant; i.e. the primary side is the same as the short circuit. Therefore, the resonant frequency f_{pon} is obtained by

$$f_{pon} = \frac{1}{2\pi\sqrt{L_{SC2} C_p}} \quad (4).$$

On the other hand, the self inductance L_2 appears at the second point is because the primary current is zero; i.e. the primary side is the same as open circuit. Therefore, the resonant frequency f_{pon} is obtained by

$$f_{poff} = \frac{1}{2\pi\sqrt{L_2 C_p}} \quad (5).$$

Thus, these resonant waveforms are generated by the capacitance C_p, which is connected in parallel with the input of the rectifier. Note that the oscillation is gradually reduced by the iron loss; resistance R_M. Using C_p and R_M the simulation waveforms agree well with the experimental waveforms including resonant frequency. Therefore, the validation of the equivalent circuit is confirmed.

III. EXPLANATION OF SECONDARY POWER OUTPUT POWER

This chapter discusses the relation between the output power P_2 and parameter of the transformer. The output power of the transformer depends on the core size and switching frequency if the number of turns in the primary side is only one-turn.

The output power P_2 is calculated by the output current I_{out2} and the output voltage E_{out2}. At first, the output current I_{out2} of the proposed circuit is introduced by a simple operation model.

Fig. 5 shows the current waveforms in the equivalent circuit. Each waveforms are shown as following; ai_1 is the primary current, which will be converted to the secondary side, i_m is the exciting current, which flows in the mutual inductance L_{m2}, and i_{out2} is the output current (instantaneous value). Note that a is the turn ratio of the transformer which is given by

$$a = \frac{N_1}{N_2} \tag{6}$$

Fig. 5 assumes that the resistance in the transformer can be neglected and the primary current is constant during one switching cycle. The exciting current is increased because the primary current commutates to the mutual inductance. Thus, the output current becomes triangle shape. The peak value of the output current is defined as aI_1.

Then the output current I_{out2} (average value for switching one cycle) is obtained by (7) from the area of the triangle waveform i_{out2};

$$I_{out2} = \frac{aI_1 t_{i2}}{2}\frac{1}{T}2 = aI_1 t_{i2} f_{sw} \tag{7),}$$

where t_{i2} is the current flow time and f_{sw} is the switching frequency.

Next, the output voltage of the proposed circuit E_{out2} is considered. The output voltage E_{out2} is given by

$$E_{out2} = L_m \frac{di_m}{dt} + L_{l2}\frac{di_2}{dt} \tag{8).}$$

Now, the differential of the current are approximately obtained by (9) and (10) from Fig. 5.

$$\frac{di_m}{dt} = \frac{aI_1}{t_{i2}} \tag{9}$$

$$\frac{di_2}{dt} = -\frac{aI_1}{t_{i2}} \tag{10}$$

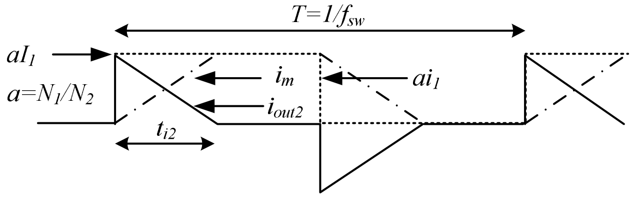

Fig.5 Current waveform of the equivalent circuit

Therefore, the output voltage E_{out2} is obtained by (11) from (8), (9) and (10).

$$E_{out2} = L_{m2}\frac{aI_1}{t_{i2}} - L_{l2}\frac{aI_1}{t_{i2}} = aI_1(L_m - l_{l2})\frac{1}{t_{i2}} \tag{11}$$

Thus, the output power P_2 of the transformer is obtained by (12) from (8) and (11).

$$P_2 = I_{out2}E_{out2} = (L_{m2} - L_{l2})(aI_1)^2 f_{sw} \tag{12),}$$

Thus the relation between the output power P_2 and the secondary side self inductance L_2 is expressed by (13) from (2), (3), and (12).

$$P_2 = (2k-1)L_2(aI_1)^2 f_{sw} \tag{13).}$$

On the other hand, the relation between the primary current I_1 and the input current for the equivalent circuit aI_1 is given by (14)

$$aI_1 = \frac{N_1}{N_2}I_1 \tag{14),}$$

where N_1 is the number of turns on the primary side and N_2 is the number of turns on the secondary side.

When the toroidal core is used in the transformer, the relation between the coil parameters and the secondary side self inductance L_2 is obtained by

$$L_2 = N_2{}^2\mu_0\mu_e\frac{A_e}{l_e} \tag{15),}$$

where μ_0 is the space permeability, μ_e is the effective permeability, A_e is the effective cross section, and l_e is the effective magnetic path length.

Thus the output power P_2 is obtained by (16) from (13), (14), and (15).

$$P_2 = (2k-1)N_1{}^2 I_1{}^2 f_{sw}\mu_0\mu_e\frac{A_e}{l_e} \tag{16}$$

Therefore, the output power P_2 is increased by the primary current I_1, the switching frequency f_{sw}, and the parameter of the core. It should be noted that the output power P_2 does not depend on the number of turns in the secondary side N_2.

IV. DESIGN OF THE ONE-TURN COIL TRANSFORMER

This chapter discusses the design of the one-turn coil transformer. In addition, an example of design example is discussed in section C.

A. The design of the one-turn coil transformer

Fig. 6 shows the design flow chart of the transformer. Each of the parameters of the transformer is decided according to the circuit specifications given in shown Fig 6.

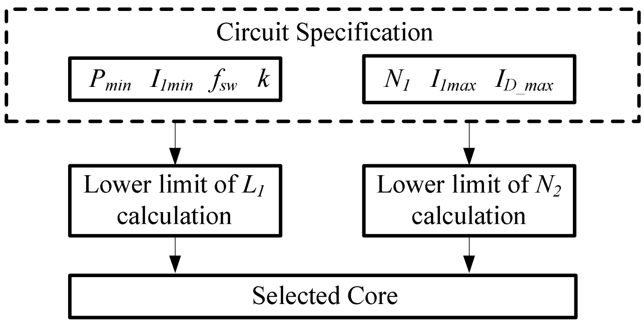

Fig.6. Design flow chart for one-turn coil.

The given circuit specifications are following; the maximum current of the main circuit is I_{1max}, the minimum current of the main circuit is I_{1min}, the switching frequency is f_{sw}, the minimum power of operation for GDU is P_{min}, and the maximum allowable current of diode for rectifier is I_{D_max}. Besides, the number of turn N_1 on the primary side is one-turn and the coupling factor k is assumed to be more than 0.9.

The design procedures of the transformer are following: First, the minimum value of the primary side self inductance L_{1min} is decided to confirm an enough power for the GDU can be obtained. Next, the number of turns N_2 is designed from the maximum current I_{D_max} of the diode rectifier. Finally, the core size of the transformer is selected according to the specifications.

B. Design method of the one-turn coil transformer

At first, the primary side self inductance L_1 is obtained by

$$L_1 = N_1{}^2 \mu_0 \mu_e \frac{A_e}{l_e} \quad (17).$$

Therefore, the relation the output power P_2 using L_1 is obtained by

$$P_2 = (2k-1) L_1 I_1{}^2 f_{sw} \quad (18).$$

Therefore, the minimum value of the primary side self inductance L_{1min} is obtained by (14) from (13) using the following components, I_{1min}, P_{min}, and f_{sw};

$$L_{1\min} \geq \frac{P_{\min}}{(2k-1) I_{1\min}{}^2 f_{sw}} \quad (19).$$

Next, the minimum turns of the secondary side winding turn N_2 is designed. The number of turns N_2 is calculated by (20) from (14) using I_{1max}, and I_{D_max};

$$N_2 \geq \frac{N_1 I_{1\max}}{I_{D\_\max}} \quad (20).$$

Finally, the core of the transformer is selected to meet (19) and (20). The value of the self inductance is decided by the only core size because the number of primary turns is constrained as only one-turn. Therefore, the core parameters should be selected by (21) from (17).

$$\mu_e \frac{A_e}{l_e} \geq \frac{L_1}{\mu_0} \quad (21)$$

The specification of the core is decided by (20) and (21)

C. The design example of the one-turn coil transformer

At first, the circuit specifications are provided. The circuit specification in Table 1 is shown as an example. The minimum value of the primary side self inductance L_{1min} is calculated by (22), on the other hand the minimum turns in the secondary side windings turn N_2 is calculated by (23).

$$L_{1\min} \geq \frac{P_{\min}}{(2k-1) I_1{}^2 f_{sw}} = 0.73\mu H \quad (22)$$

$$N_2 \geq \frac{N_1 I_{1\max}}{I_{D\_\max}} = 12 \quad (23)$$

Therefore, the core that meets the conditions in (22) and (23) is selected. As a result, we fined the core, which has parameters as follows; A_e=150 mm^2, l_e=56.5 mm, and μ_e=229. Using this core, L_1 of 0.79 µH is obtained with N_2 of 12 turns.

D. Evaluation of the analysis results

The analysis results are evaluated by a basic experimental circuit in Fig. 1. The transformer was used in the experimental, which was designed in the previous chapter.

Fig. 7(a) shows the relation between the output power P_2 and the number of turns in the secondary side which is obtained by the experimental results. Note that the output power P_2 is increasing as the N_2 increased. This reason is because of the coupling factor k is changed by N_2.

On the other hands, Fig. 7(b) shows the relation between the number of the secondary winding turn and the value of the output power P_2 divided by (2k-1) to exclude the variation of k. Then, the output power is standalone from the number of turns on secondary side while the coupling factor is constant.

Fig. 8 shows the relation between the output power P_2 and the primary current based on the experimental result and the theoretical analysis from (18). The output power is increasing according to the primary current.

TABLE I. CIRCUIT SPECIFICATIONS.

I_{1min}	I_{1max}	f_{sw}	P_{min}	I_{D_max}	k
7.2A	24A	10kHz	0.3W	2A	0.9

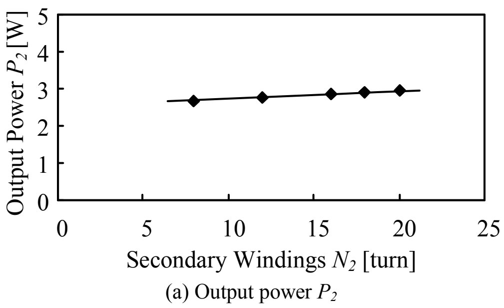

(a) Output power P_2

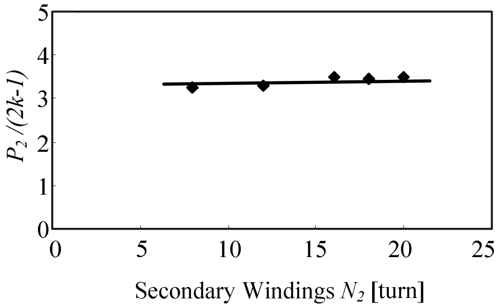

(b) Output power divided by (2k-1)

Fig. 7. Characteristics of the number of turns in the secondary side (f_{sw}=10 kHz, N_2=vary, *Duty*=35%, I_{out1}=21 A)

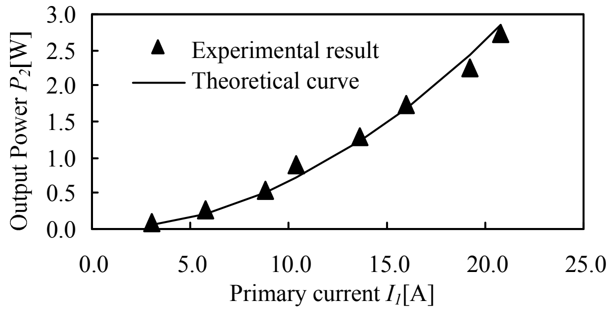

Fig.8 Output power P_2 according to the main circuit current. (f_{sw}=10 kHz, N_2=12turn, *Duty*=35%, R_l=changing)

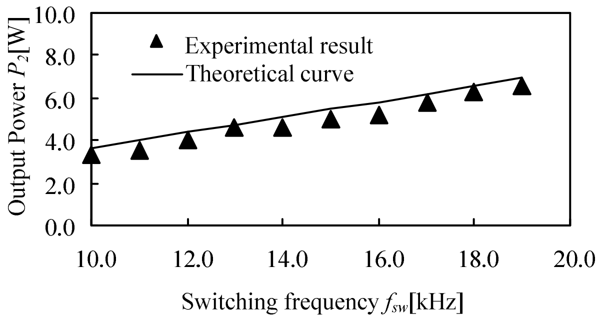

Fig. 9. Output power P_2 according to the switching frequency (N_2=12 turn, *Duty* = 35% , I_{out1}=23.5 A)

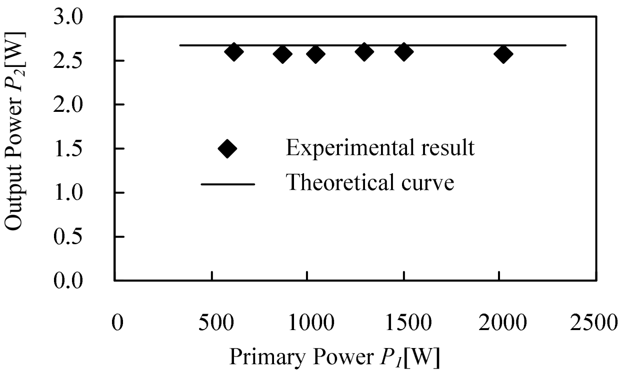

Fig. 10. Output power P_2 characteristic by changing the P_1.

(f_{sw}=10 kHz, N_2= 12turn, *Duty*=35%, I_{out1}=20 A, E_{in}=changing)

Fig. 9 shows the relation between the output power P_2 and the switching frequency. Fig. 9 confirms that the proposed method could obtain an enough output power P_2 to operate the GDU. It is noted that the GDU only requires the power of a few watt (0.3W) to drive the power device.

Fig. 10 shows the output power P_2 with the output power of the main circuit. The output power P_2 is not increase even the output power of the main circuit has been increased. The output power of the main circuit is controlled by the DC link voltage. Therefore, the output power of the gate power supply does not depend on the active power of the main circuit.

In each result, the experimental results agreed with the theoretical line. In addition, these experimental verifications concluded that the proposed self-supplying power circuit could generate enough power to operate the GDU. Besides, the output power of the gate power supply is increased by a larger primary current or a higher switching frequency even the output power of the main circuit is still kept small.

V. Evaluation of the Proposed Circuit as a Gate Power Supply

A. *Fundamental operation in a DC chopper*

Fig. 11 shows the evaluation circuit of the proposed circuit. In this chapter, the operation of a GDU using the proposed power source circuit will be confirmed by the experiment circuit. The power consumption of a GDU is 0.35 W, and the operation voltage is more than 24 V. When the output voltage of the proposed gate power circuit is less than 24 V, an auxiliary DC power source (e_{sub2}) is used for the initial operation. It should be noted that when the DC

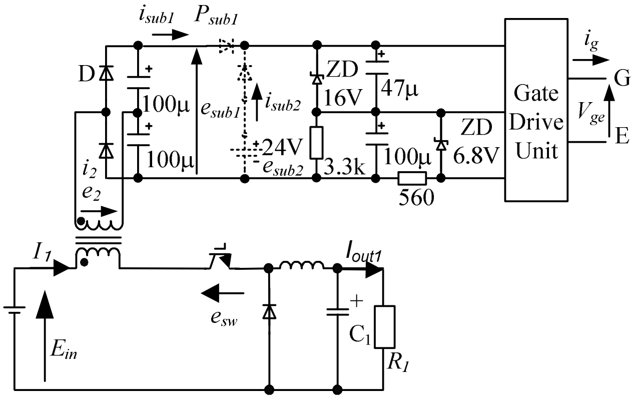

Fig. 11. Experiment circuit of self-supplying power circuit.

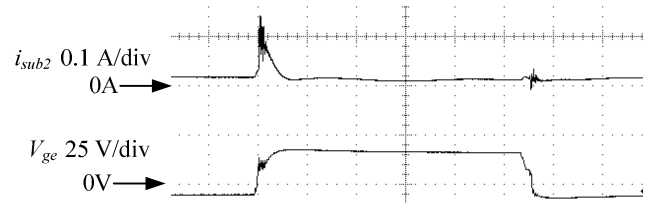

(a) Current from sub supply e_{sub2} and output voltage of the GDU V_{ge} without proposed circuit

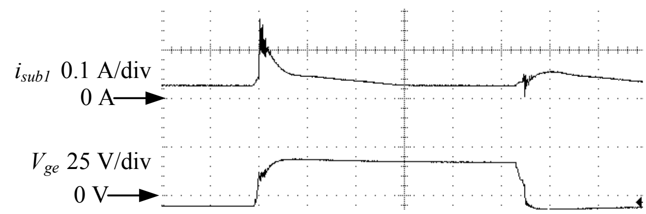

(b) Current from proposed circuit and output voltage of the GDU V_{ge} with proposed circuit

Fig. 12 Operation waveforms of the GDU using the proposed circuit at step down chopper

power supply current i_{sub2} is equaled to zero, this means that only the proposed circuit supplies the power to the GDU. The gate voltage is designed as 16 V for on-state period and –7 V for off-state period respectively.

Fig. 12 shows the operation waveforms of the GDU with using the proposed power circuit; V_{ge} is the voltage between the gate and emitter, the supply current i_{sub1} is from the proposed circuit and the current i_{sub2} is from the sub power supply. The experimental conditions are following; the output current of step-down chopper I_{out1}=7.8A, the frequency of the switching device f_{sw}=16kHz, the switching duty ratio=35%. In Fig. 12(a), the current for the GDU is supplied from the sub power supply e_{sub2} without the proposed circuit. On the other hands, in Fig. 12(b), the current for the GDU is i_{sub1} from the proposed circuit. The same gate voltage waveforms are obtained in Fig. 12(a) and (b). These results confirmed that the proposed circuit is able to supply enough power for the GDU initially and operate normally onwards.

B. *Connection point in a Three-phase inverter*

Fig. 13 illustrates several connection points of the transformer in a three-phase inverter. In the previous fundamental verification, the self-supplying transformer is connected in series to the switching device. Practically, the

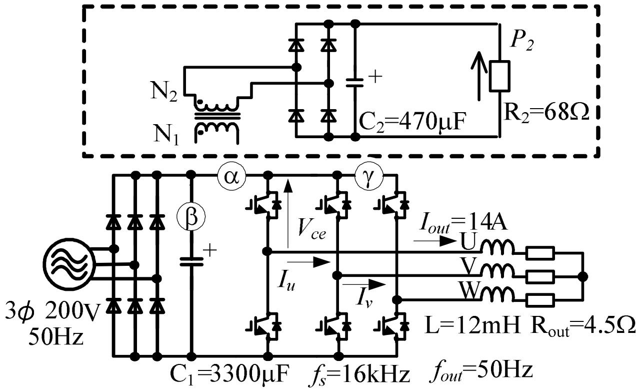

Fig. 13. The possible connection points of the transformer in a three phase inverter.

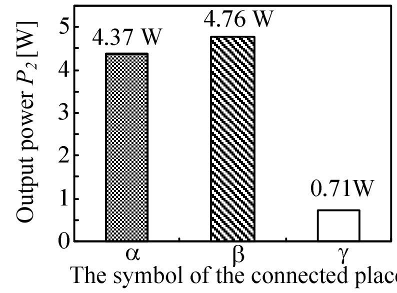

Fig. 14. Output power P_2 at the selected connection point of the transformer.

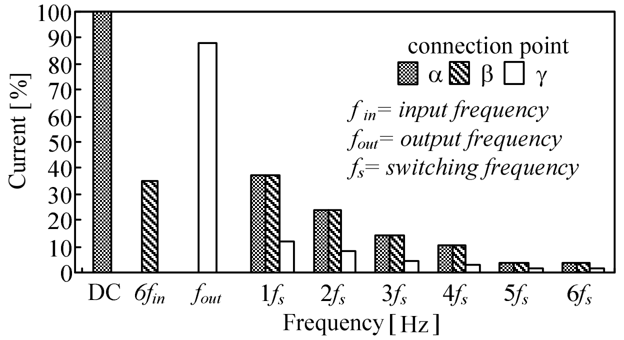

Fig. 15. Harmonics components of the primary current at each connection point.
(The reference value is in DC current at connection point α)

transformer can be connected in series to (α) the DC-link part, (β) the smoothing capacitor, or (γ) the current of each leg in order to reduce the cost.

Fig. 14 shows the output power P_2 of the secondary side according to the connected location of the transformer. The output power P_2 obtains more than 4 W when the primary side of the transformer is connected to the point (α) and (β). The proposed gate power circuit is able to supply enough power to operate up to six GDUs. On the other hand, the proposed circuit can be only generated 0.71W when the primary side of the transformer is connected to the point (γ).

Fig. 15 shows the harmonics components of the primary current at each connection point. The harmonics components of the switching frequency at the point (γ) are smaller than other connection points as shown in Fig. 13. In addition, a same output power is obtained by the proposed circuit when the primary side is connected to the point (α) and (β) because the output power is dominated by the harmonics components of the switching frequency in the primary current. It should be noted that the output power P_2

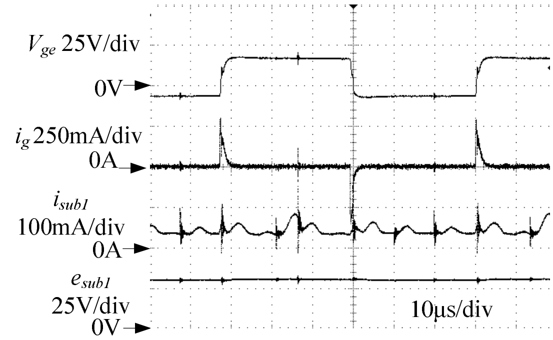

Fig. 16. Operation waveforms of the GDU with the proposed circuit

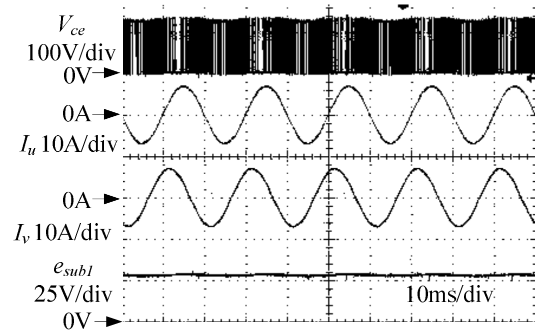

Fig. 17. Operation waveforms of the inverter with the GDU using the proposed circuit

is proportional to the switching frequency and the square of the primary current as shown in (16). However, the connection point (α) faces the magnetic saturation from the current at the DC component of the main circuit. Therefore, a large core is required for the transformer if connecting at this point. Because of these reasons, the connection point (β) is the best connection point because point β can obtain the largest power and use a smaller core.

C. Application in a three-phase inverter

In this section, the performance of the gate drive unit will be evaluated. A three-phase inverter is used as the main circuit, and the GDU is supplied by the proposed gate power circuit. Note that only the GDU for U-phase is supplied by the proposed gate power circuit where the primary side of the transformer is connected to point (β).

Fig. 16 shows the operation waveforms of the proposed circuit in Fig. 13. Start from the top, V_{ge} is the voltage between the gate and emitter; i_g is the gate current, i_{sub1} is the supply current for the GDU and e_{sub1} is the power supply voltage for the GDU. The power supply voltage e_{sub1} is at constant while the gate current i_g is operated in charge or discharge mode. Besides, the actual gate voltage almost agrees with the design value. It is noted that the auxiliary power source did not work in this situation because the output voltage of the auxiliary power source is up to 24 V only; however the power supply voltage is kept to 27 V. The voltage between the gate and the emitter does not contain a large distortion. Therefore the GDU is then confirmed to operate normally even if the proposed power supply is used.

Fig. 17 shows the operation waveforms of the three-phase inverter which are the collector-emitter voltage of the switching device e_{sup}, the U phase current I_u , the V phase

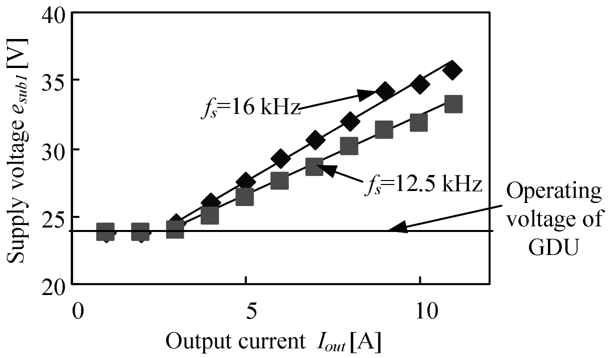

(a) Gate power supply voltage according to the output current.

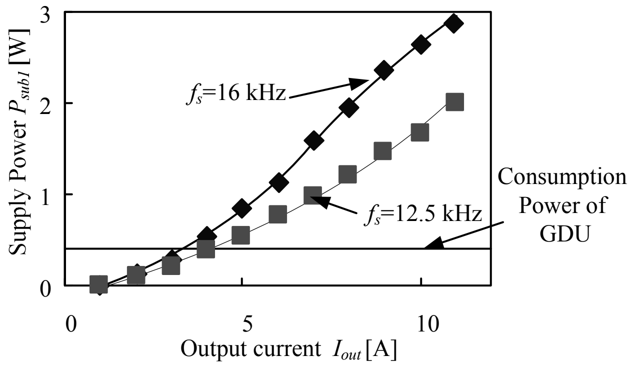

(b) Output power of the gate power supply according to the output current.

Fig. 18. The relationships between the three-phase inverter circuit and the gate power circuit

current I_v, and the power supply voltage $e_{sub1}$for the GDU. Sinusoidal current waveforms are obtained in U-phase and V-phase and without any distortion. Besides, the gate power supply shows a constant voltage. Therefore, the results confirmed that the inverter is able to operate normally by using the GDU with the proposed gate power circuit.

Fig. 18(a) shows the relations between the output current of the main circuit with the supply voltage e_{sub1} of the GDU and Fig. 18(b) shows the relations between the output current of the main circuit with supply power P_{sub1} of the GDU. Two switching frequency of 16 kHz and 12.5 kHz were tested to investigate the influence of the switching frequency. The results confirmed that the GDU can be operated by the proposed gate power circuit when the output current is more than 4A. It should be noted that the gate power supply voltage increases when the output current is larger. This reason is that the output power of the transformer is higher than the power consumption of the GDU. Therefore, the proposed gate power circuit should be designed in a way that the gate power supply voltage is at the maximum load condition and the switching frequency is lower than the absolute operation voltage of the GDU.

VI. CONCLUSION

This paper proposed a self-supplying gate power circuit for the gate drive unit which is using a one-turn transformer. The characteristics of the proposed gate power circuit are confirmed by the experimental results as following;

(i) The secondary power is almost proportional to the primary current and its frequency. On the other hands, the active output power for the load does not influence the gate drive performance.

(ii) The primary side of the transformer should be connected in series to the smoothing capacitor at the DC link of the inverter in order to reduce the core size and to obtain the maximum power.

(iii) The same gate voltage is obtained by the proposed circuit in comparison to that of a conventional gate drive unit.

(iv) The proposed gate power supply circuit is applied to a three-phase inverter, and sinusoidal output current waveforms are obtained as similarly to the conventional inverter.

As a result, the validity of the proposed self-supplying gate power circuit is confirmed.

In future study, the effect of the noise reduction will be investigated in the proposed circuit because the rise time of the switch current is reduced by the series transformer. In addition, the initial operation of the proposed circuit without the auxiliary power supply will be considered.

REFERENCES

[1] John, V.; Bum-Seok Suh; and Lipo, T.A.; “High-Performance Active Gate Drive for High-Power IGBT's”, IEEE Transactions on Industry Applications, Vol. 35, Issue. 5, pp. 1108-1117, Oct. 1999

[2] Kaiwei Yao; and Lee, F.C.; “A novel resonant gate driver for high frequency synchronous buck converters”, IEEE Transactions on Power Electronics, Vol. 17, Issue.2, pp.180-186, Mar. 2002

[3] Wiegman, H.L.N.; “A resonant pulse gate drive for high frequency applications”, Seventh Annual Applied Power Electronics Conference and Exposition, Boston, MA, pp. 738-743, Feb.1992

[4] Zhihua Yang; Sheng Ye; and Yan-Fei Liu; “A New Dual-Channel Resonant Gate Drive Circuit for Low Gate Drive Loss and Low Switching Loss”, IEEE Transactions on Power Electronics, Vol. 23, Issue. 3, pp. 1574-1583, May. 2008.

[5] International Rectifier, “Application note AN-978: HV Floating MOS-Gate Driver ICs”, Mar. 2007. [Online]. Available: http://www.irf.com/technical-info/appnotes/an-978.pdf. [Accessed: May. 2008]

[6] J.Adams; “Design Tip: Bootstrap Component Selection For Control IC’s”, 4. Sept. 2001. [Online]. Available: http://www.irf.com/technical-info/designtp/dt98-2.pdf. [Accessed: May. 2008]

[7] Shihong Park; and Jahns, T.M.; “A self-boost charge pump topology for a gate drive high-side power supply”, IEEE Transactions on Power Electronics, Vol. 20, Issue. 2, pp. 300-307, Mar. 2005.

[8] Moe. Imaizumi and Yukihiko. Sato, “Application and evaluation of floating methods for gate drive power supplies, IEEJ on Semiconductor Power Conversion, SPC-08-19, pp.49-54, Jan. 2008. [In Japanese]